Article

Estimation of Leaf Area Index in a Typical Northern Tropical Secondary Monsoon Rainforest by Different Indirect Methods

Xiansheng Xie [1,2,3], Yuanzheng Yang [1,2], Wuzheng Li [4], Nanyan Liao [4], Weihu Pan [4] and Hongxin Su [1,2,*]

1 Key Laboratory of Environment Change and Resources Use in Beibu Gulf (Ministry of Education), Nanning Normal University, Nanning 530001, China
2 Guangxi Key Laboratory of Earth Surface Processes and Intelligent Simulation, Nanning Normal University, Nanning 530001, China
3 Research Institute of Forestry Policy and Information, Chinese Academy of Forestry, Beijing 100091, China
4 Guangxi Fangcheng Golden Camellia National Nature Reserve, Fangchenggang 538021, China
* Correspondence: hxsu@nnnu.edu.cn

Abstract: The leaf area index (LAI) is a crucial indicator for quantifying forest productivity and community ecological processes. Satellite remote sensing can achieve large-scale LAI monitoring, but it needs to be calibrated and validated according to the in situ measurements on the ground. In this study, we attempted to use different indirect methods to measure LAI in a tropical secondary forest. These methods included the LAI-2200 plant canopy analyzer (LAI-2200), Digital Hemispherical Photography (DHP), Tracing Radiation and Architecture of Canopies (TRAC), and Terrestrial Laser Scanning (TLS) (using single-station and multi-station measurements, respectively). Additionally, we tried to correct the measured LAI by obtaining indicators of woody components and clumping effects. The results showed that the LAI of this forest was large, with estimated values of 5.27 ± 1.16, 3.69 ± 0.74, 5.86 ± 1.09, 4.93 ± 1.33, and 3.87 ± 0.89 for LAI-2200, DHP, TRAC, TLS multi-station, and TLS single-station, respectively. There was a significant correlation between the different methods. LAI-2200 was significantly correlated with all other methods ($p < 0.01$), with the strongest correlation with DHP ($r = 0.684$). TRAC was significantly correlated with TLS single-station ($p < 0.01$, $r = 0.283$). TLS multi-station was significantly correlated with TLS single-station ($p < 0.05$, $r = 0.266$). With the multi-station measurement method, TLS could maximize the compensation for measurement bias due to the shadowing effects. In general, the clumping index of this forest was 0.94 ± 0.05, the woody-to-total area ratio was $3.23 \pm 2.22\%$, and the total correction coefficient was 1.03 ± 0.07. After correction, the LAI estimates for all methods were slightly higher than before, but there was no significant difference among them. Based on the performance assessment of existing ground-based methods, we hope to enhance the inter-calibration between methods to improve their estimation accuracy under complex forest conditions and advance the validation of remote sensing inversion of the LAI. Moreover, this study also provided a practical reference to promote the application of LiDAR technology in tropical forests.

Keywords: effective leaf area index; secondary forests; optical instruments; terrestrial laser scanning

1. Introduction

As the most structurally complex forest ecosystem on land, tropical forests cover about 10% of the Earth's surface and about 45% of the total global forest area [1]. They contain more than 50% of the world's known species, and their carbon stocks are about half of the global vegetation carbon stocks, which play a key role in maintaining biodiversity, the global carbon cycle, and climate change mitigation [2,3]. With anthropogenic disturbances, more and more primary tropical forests are disappearing and transforming into secondary forests in different stages, whose canopy structure and species composition have changed significantly [4]. The canopy is the most dominant and active site of forest interaction with the external environment. As the core element, the leaf is the main carrier of its physiological

processes with the atmosphere, such as energy and water exchange, which controls carbon uptake and plant productivity [5,6]. The leaf area index (LAI) is usually defined as half the total intercepting area per unit ground surface area and is a dimensionless variable [7]. It describes the intercepted area of photosynthetically active radiation by plants and is a key indicator for effectively quantifying forest productivity and community ecological processes, which is considered an indispensable input parameter in regional or global vegetation dynamics models [8]. Therefore, it is important to accurately estimate tropical forest LAI to understand tropical ecosystem processes [9,10].

Traditional passive remote sensing techniques can achieve landscape and regional-scale LAI estimation, but they need to be calibrated and validated according to the in situ measurements on the ground [11]. LAI field measurement methods are mainly divided into direct and indirect methods. Direct methods commonly include destructive sampling, leaf-litter collection, and allometric relationship methods [8,12]. The destructive sampling method is harmful to trees and can only be used in small areas, while the leaf-litter collection and allometric relationship methods are easily influenced by location, species, and season, with many uncertainties in the measurement process [13,14]. Indirect methods characterize forest canopy structure mainly through gap fraction to achieve LAI inversion [15]. Due to the advantages of fast and non-destructive measurements, traditional optical instruments have been widely used to estimate LAI at the plot-scale, such as the LAI-2200 plant canopy analyzer (LAI-2200), Tracing Radiation and Architecture of Canopies (TRAC), DEMON, CI-110 plant canopy imager, Digital Hemispherical Photography (DHP) [5,16]. Terrestrial laser scanning (TLS) opens new paths for measuring LAI by launching and recycling laser signals to form massive 3D data, providing more details on the forest canopy's vertical structure and terrain [17]. With the direct method as a control, some studies have shown that there was a strong correlation between LAI-2200, DHP, TRAC, and TLS for the LAI estimation, with differences of about 10–50% for each [5,8,18,19]. The LAI-2000 (the base version of the LAI-2200) and TRAC underestimated, on average, 30% when measuring LAI [20,21], but could achieve 80% accuracy with careful handling [22]. Zou et al. [23] conducted a comprehensive validation assessment of DHP using a sampling method and found that it mostly underestimated by about 20%. The TLS was able to maintain a consistent correlation with the LAI-2200, and its estimation was well within the range of possible bias of the LAI-2000 [24,25]. It would be hard to draw definite conclusions from method comparisons if the uncertainty of the control values was relatively large.

The reasons for the estimation bias of these ground-based indirect methods originate, in large part, from their assumptions. (1) Leaves are assumed to be black (impervious to light) and cannot effectively distinguish between leaf and non-leaf elements, such as trunks and branches, and measurements will include woody component contributions; (2) leaves are assumed to be randomly distributed in most of the methods, except TRAC. In fact, leaves tend to be clumped, and LAI is easily underestimated, especially in compound forests [26,27]. The output of these methods should be called the effective Plant Area Index (PAI) or effective LAI [28]. To address the above issues, scholars commonly quantify the woody components and clumping effect by using the woody-to-total area ratio and clumping index, respectively. At present, methods for measuring the woody-to-total area ratio can be classified into three types: the destructive sampling method, the background method, and the Photoshop method [29,30]. The clumping index can be calculated by the LX method (based on the logarithmic gap fraction averaging method), the CC method (based on the logarithmic gap size averaging method), and the CLX method (combined with the LX and CC methods) [27]. It can be obtained quickly by TRAC (based on the CC method).

In general, natural forests in the tropics have high species richness and complex canopy structures, which are considered to have a high LAI [9,31]. In tropical humid evergreen forests, measuring LAI relies almost completely on indirect methods and is extremely difficult through direct methods [32]: (1) Due to forest protection policies, it is difficult to obtain leaves by the destructive sampling method; (2) evergreen forests

lack a significant deciduous period, so the leaf-litter collection method is not applicable; (3) the diversity of tree species makes it difficult to obtain the optimal allometric equation, and it is also necessary to calculate the specific leaf area for each tree species rather than calculating the average of multiple species. Some studies have compared the suitability of one or more traditional optical instruments for measuring LAI in tropical deciduous and tropical humid evergreen forests and proposed corresponding correction schemes based on instrument characteristics [18,19]. Some studies have also attempted to measure tropical forest LAI using the TLS technique, but the results were not very satisfactory due to the shadowing effect [33,34]. Compared to temperate and boreal zones, LAI data are less available in the tropics, with only 8% of observations in the global LAI database from tropical biomes [35,36]. This indicates the complexity of the LAI field measurements and product validation in tropical forests.

Even though the LAI field measurement is limited to a small scale, it still forms the basis of all LAI validation studies. For complex tropical forests, the more difficult it is to obtain the true LAI by direct methods, the more important it is to pay attention to the differences in the estimation of ground-based indirect methods, because it is a prerequisite for calibrating these methods and establishing uniform measurement protocols. Only if these methods can provide more accurate ground verification data will inversion of LAI at a larger scale become possible. In China, tropical rainforests and monsoon forests reach the northernmost limits of the world and are typical and representative [37,38]. However, there is still a great lack of LAI studies in tropical monsoon rain forests. In view of this, this study carried out field measurements in the southern foothills of the Shiwan Mountains in Guangxi, China, and attempted to compare the differences in LAI estimation by LAI-2200, DHP, TRAC, and TLS in a northern tropical secondary monsoon rainforest at the plot scale. Considering the effects of woody components and clumping effects, this study compared the differences before and after correction by obtaining the corresponding parameters. We hoped to promote their application in similar stand environments and provide a practical example for tropical forests.

2. Materials and Methods

2.1. Study Area

The study area is located in the Fangcheng Golden Camellia National Nature Reserve in Guangxi, China (Figure 1). The reserve aims to protect the rare and endangered Golden Camellia and the northern tropical forest ecosystem on which they depend for survival. It belongs to the Lanshan branch of the Shiwan Mountains, with coordinates of 21.7511°N–21.7541°N, 108.1177°E–108.1236°E and a total area of 9195.1 hm^2. The area has a tropical monsoon climate. Due to its close proximity to the coast of the Beibu Gulf, ocean winds prevail, and the average annual precipitation can reach more than 2900 mm. The average annual temperature is 21.9 °C, and ≥10 °C accumulated temperature is 8100 °C. The regional zonal vegetation is the northern tropical monsoon rainforest and distinctive valley rainforest, which are both evergreen broad-leaved forests. The monsoon rainforest is dominated by trees such as *Madhuca pasqueri*, *Machilus chinensis*, *Sloanea sinensis*, and *Sterculia lanceolata*, while the valley rainforest is dominated by *Hopea chinensis* as the signature species. Because of the long history of human activities, the area of primary forests has been seriously reduced and mostly exists in the form of secondary forests.
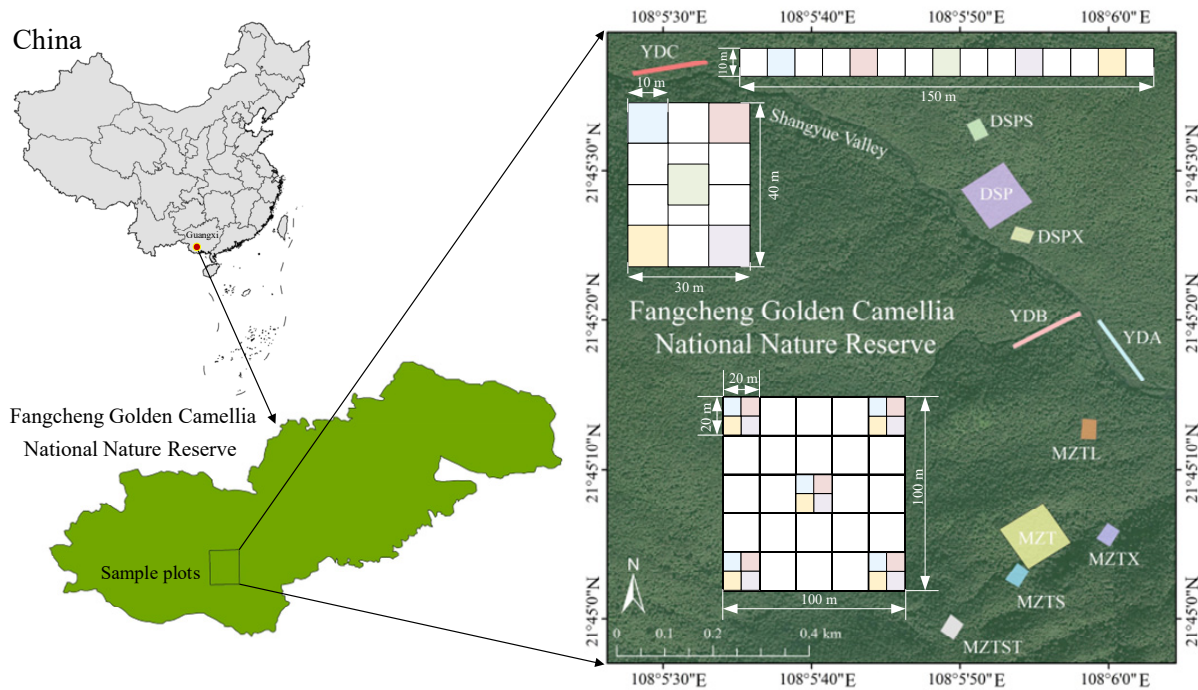
Figure 1. Location of the study area.

2.2. Measurement Principle

In essence, the LAI inversion based on the gap fraction is implemented by following the Beer–Lambert law, which simulates the process of solar rays passing through the tree canopy. The principle is as follows:

$$T(\theta) = e^{-\frac{G(\theta,\alpha)\text{LAI}}{\cos(\theta)}} \tag{1}$$

where $T(\theta)$ is the gap fraction, $G(\theta,\alpha)$ is the projection function, θ is the solar incidence angle, and α is the average leaf angle.

The measurement of traditional optical instruments is a process based on the solar rays (visible light) being sensed by the sensors. The sensor of the LAI-2200 is a fisheye lens with a field of view of 148°, which includes five rings with central zenith angles of 7°, 23°, 38°, 53°, and 68°. Additionally, its optical filter restricts the radiation incoming to the 320–490 nm wavelength band (blue light). The sensor of the DHP is a fisheye lens with a field of view of 180°, and it images the entire hemispherical space projected on the image level by a digital camera (the wavelength band range is not limited). TRAC consists of three photosynthetically active radiation (PAR, 400–700 nm) sensors, which measure the transmitted direct light in the sun's direction [26,39]. The TLS regards the launched laser signal (light beam) as a solar ray, and the LAI inversion is achieved by classifying and counting the recycled point cloud data [40]. In this study, the estimated LAI by TLS is based on the contact frequency method, calculated as the probability of a beam penetrating the canopy and encountering a vegetative element [17]. The contact frequency $N(\theta)$ between a light beam and vegetation element in the direction (θ) is given by:

$$N(\theta) = G(\theta)\frac{\text{LAI}}{\cos(\theta)} \tag{2}$$

For the contact frequency of the layer, it can be calculated by:

$$N(s) = \frac{n_I(s)}{n_I(s) + n_p(s)} \tag{3}$$

where $N(s)$ is the contact frequency of light beams in the sth layer, $n_I(s)$ is the number of light beams intercepted by the sth layer, $n_p(s)$ is the number of light beams passing through the sth layer, and $n_I(s) + n_p(s)$ is the total number reach the sth layer.

The LAI of the sth horizontal layer within the canopy can be calculated by:

$$\text{LAI}(s) = N(s)\frac{cos(\theta)}{G(\theta)} \tag{4}$$

where $\text{LAI}(s)$ is the LAI of the sth horizontal layer within the canopy.

Thus, the LAI of the entire tree is calculated by sum of $\text{LAI}(s)$ as follows:

$$\text{LAI}_{total} = \sum_{s=1}^{s} \text{LAI}(s) \tag{5}$$

2.3. Sample Plot Selection

To maintain biodiversity and promote long-term observation of rare plants such as *Golden camellia* and *Hopea chinensis*, two 100 m × 100 m sample plots, six 30 m × 40 m sample plots, and three 10 m × 150 m sample strips were set in the reserve. In this study, based on the five-point sampling method, five sub-sample plots of 20 m × 20 m size were selected in the 100 m × 100 m sample plots, and five sub-sample plots of 10 m × 10 m size were selected in the 30 m × 40 m sample plots. Based on the equidistant sampling method, five sub-sample plots of 10 m × 10 m size were selected in the sample strips (Figure 1). The naming of the sample plots was based on Chinese abbreviations and was intended to distinguish them. For example, "YDA" indicated "Yangdai A", "DSP" and "MZT" were named based on the place names "Dashiping" and "Meizaitian", and the rest of the sample plots were distinguished by adding the letters "S", "X", "L", and "ST" according to their relative positions to "DSP" and "MZT". With the size of 10 m × 10 m as the measurement unit, a total of 85 samples were obtained. Differential GPS signals were received by HyperGIS (HowayGIS, Shanghai, China) at the four boundary points of each sample plot to locate its coordinates and obtain altitudes. The average value of the altitude of the boundary points was considered the sample plot altitude. From this, we could obtain the elevation difference between the two sets of top and bottom points, and combined with the sample plot size (projected distance), the slope degree (average of two sets of data) could be calculated. The slope aspect was obtained by the operator standing at the top of the plot, facing the bottom, keeping parallel to the boundary, and measuring with a hand-held compass.

According to the data of the previous plant survey of the reserve, the area had suffered from mountain fire deforestation. Most of the trees in all sample plots belonged to the small diameter class, with a high number of individuals less than 5 cm in diameter at breast height and a limited number of mature individuals. Tree heights were mainly concentrated between 4–7 m. The stands were similar in age between different plots, all at a young stage (about 20–30 years). The canopy density ranged from 0.38 to 0.56 (Table 1). The shrub layer in the sample plots was not developed, but mixed with a variety of tree seedlings. The herbaceous layer was sparse, with a cover of 8–10% and an average height of about 0.35 m.

Table 1. The basis information of sample plots.

Name	Size (m)	Number of Sub-Sample Plots	Altitude (m)	Slope Aspect (°)	Slope Degree (°)	Mean DBH (cm)	Mean Tree Height (m)	Canopy Density
YDA	10 × 150	5	92	150	10	4.45	5.62	0.40
YDB	10 × 150	5	117	260	25	7.17	6.69	0.50
YDC	10 × 150	5	209	70	15	5.68	6.63	0.38
DSPS	30 × 40	5	169	210	28	6.13	6.35	0.47
DSPX	30 × 40	5	124	200	18	6.03	6.17	0.56
MZTL	30 × 40	5	132	20	15	6.45	6.33	0.53
MZTX	30 × 40	5	147	60	23	5.73	6.31	0.48
MZTST	30 × 40	5	278	35	22	5.02	6.06	0.43
MZTS	30 × 40	5	210	29	24	5.95	6.69	0.45
DSP	100 × 100	20	139	135	23	6.42	6.55	0.50
MZT	100 × 100	20	190	60	34	7.28	6.31	0.55

Note: DBH indicates diameter at breast height. The slope aspect is expressed as a positive number between 0° and 360°. North, East, South, and West are 0° (360°), 90°, 180°, and 270°, respectively.

2.4. Field Measurements

Considering the large uncertainty in results when measured at the beginning and end of forest growth [41], the data collection time for this study was chosen to be conducted in the summer (August 2021). This was during the peak growing season of the forest, when the leaves were fully extended. To enhance the comparability of the data, we strictly followed the instructions of each measurement method to ensure that they were applied under ideal sky conditions and that the data were acquired at the same height (1.5 m) on the ground. Instead of measuring the LAI of individual trees, we measured the LAI of the forests (plot scale). Considering the measurement characteristics of the different methods, we used sub-sample plots as the basic unit. This configuration allowed maximum coverage with each method with a minimum overlap and ensured that the estimated LAI was from the trees within the plot. Since the requirements of the different methods were different, the measurements were not always carried out at exactly the same locations, but the final measurements could all be compared on a scale of 10 m × 10 m. The measurement schemes for the different methods were as follows:

2.4.1. LAI-2200

Measurements were taken synchronously using two LAI-2200 instruments (LI-COR, Lincoln, NE, USA) under a stable cloudy condition (no direct light). Before the measurement, the two instruments were time-synchronized, and matching files were created to achieve uniform measurement standards. One of them was placed in the open space outside the forest to automatically record the A-values (considered as measured values above the canopy) at a 30 s frequency, with the instrument facing the same direction as the sample plot. The other one was taken inside the forest to measure five B-values (measured values below the canopy) along the Z-shaped route (Figure 2a), keeping the height at about 1.5 m. This ensured that the B-values were evenly distributed among the sub-sample plots and that the measurement results were more representative. A 90° view cap was placed on both instruments to eliminate the effects of residual direct light and the operator itself. After the measurement, the software FV2200 v2.1 was used to match the time series of A-values and B-values and insert the A-values of the adjacent time into the corresponding B-values. The average value of LAI for the five measurement points was calculated as the result of this plot.
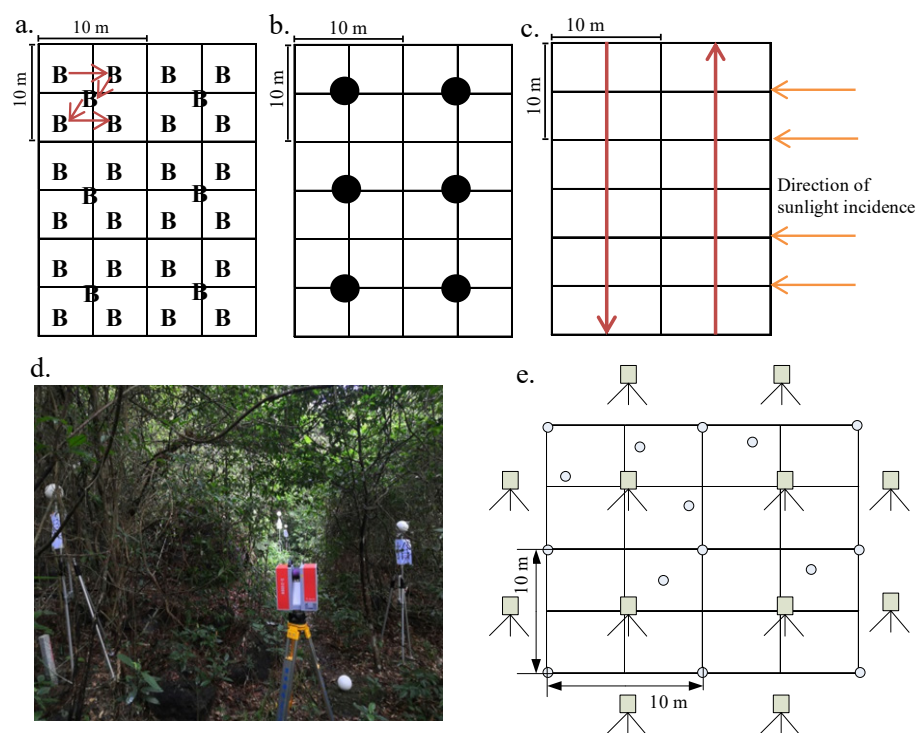
Figure 2. Measurement schemes for obtaining LAI by different indirect methods. (**a**) Measurement route of LAI-2200 B-value; (**b**) Camera shooting point for DHP; (**c**) Measurement route for TRAC; (**d**) Field measurement scenes for TLS; (**e**) Instrument and target ball site locations for TLS.

2.4.2. DHP

Measurement was carried out using HemiView (Delta-T, Cambridge, UK). The instrument was composed of a digital camera (Canon EOS 70D), a fisheye lens (Sigma EX-DC 4.5 mm), and an SLM8 auto-balancing bracket. The measurement time and sky condition were consistent with the LAI-2200. The camera was installed on the balance bracket with the fisheye lens facing upwards vertically (about 1.5 m above the ground), the exposure mode was set to auto, the shutter speed was set to 1/125 s, and the resolution was set to "High" (size = 5472 × 3648, about 20 mega pixels). It was placed in the center of the sample plot to take images of the canopy (Figure 2b). Data pre-processing was performed by the software Sidelook v1.1.01 (http://www.appleco.ch, accessed on 18 January 2022) to obtain classification thresholds for the sky and canopy. The LAI calculation was completed in the software HemiView v2.1.1.

2.4.3. TRAC

TRAC-III (Wave Engineering, Nepean, ON, Canada) was chosen to be used for measuring, in a clear and sunny condition. For the measurement, it was placed horizontally (about 1.5 m above the ground) and moved at a uniform speed of 0.33 m/s, keeping the direction perpendicular to the direction of sunlight incidence (Figure 2c). When an obstacle was encountered, the operator pressed the control key once, briefly, to insert a time label and start recording a new data segment. Once the obstacle was crossed, a time label was inserted again so that useless data segments could be discarded during the calculation. Each sampling line was measured reciprocally, with a time label inserted at 10 m intervals. The average of the two results was taken as the final LAI value. The data were processed by the software TRAC Win v5.9.0.

2.4.4. TLS

The Scanning System S-3180 laser scanner (PENTAX, Saitama, Japan) was used for field data acquisition (Figure 2d). To analyze the influence of shadowing effects on TLS,

single-station and multi-station measurements were used. The boundary points and the inside of the sample were placed with some target balls, aiming to ensure that more than three target balls could be seen simultaneously between any two scanning stations, which facilitated data cropping and merging. The instrument scan quality was set to "Normal" (duration of scan: ca. 3 min. 22 s.), and the resolution was set to "High" (6.3 mm within 10 m) to ensure that the scan covered the entire plot area. The point cloud data was acquired by setting up stations at different locations (Figure 2e). The data acquired at the center (TLS single-station) and the merged multi-station data (TLS multi-station) were processed, respectively. Pre-processing work, such as denoising, was completed by the software Z + F Laser Control v8.8.0 (Zoller+Fröhlich GmbH, Wangen im Allgäu, Germany). Registration, merging, ground point filtering (the height threshold was set to 1.5 m), normalization, and calculation of LAI were completed in the software LiDAR 360 v4.0 (Green Valley, Beijing, China). Except for the merging, the consistency of the data processing process between TLS multi-station and TLS single-station was maintained, including steps and parameter settings, etc.

2.5. Correction Methods

The correction was applied using the formula proposed by Chen et al. [42], as follows:

$$\mathrm{LAI}_c = \frac{(1-\alpha)}{\Omega}\mathrm{LAI}_e \tag{6}$$

Let $\lambda = \frac{(1-\alpha)}{\Omega}$, then $\mathrm{LAI}_c = \lambda\mathrm{LAI}_e$.
where LAI_c is the corrected LAI, LAI_e is the effective LAI (uncorrected), and λ is the total correction coefficient, which consists of the woody-to-total area ratio (α) and the clumping index (Ω). If $\lambda > 1$, it means that an "upward" correction is needed, where the degree of overestimation caused by the woody component is less than the degree of underestimation caused by the clumping effect. Ω could be obtained simultaneously when the effective LAI was measured by TRAC. Referring to the PS method proposed by Qi et al. [29], the clone stamp tool in Photoshop was used to remove the woody components from the images taken by DHP to calculate α:

$$\alpha = (L_1 - L_2)/L_1 \tag{7}$$

where L_1 is the LAI calculated by HemiView software when the wood component was not removed, and L_2 is the LAI calculated again after removal.

2.6. Data Analysis

Based on the software IBM SPSS Statistics v22, the one-way ANOVA was performed on the LAI measured by different methods, and the correction indices were obtained from different plots, using the LSD method to test the significance of differences. A Pearson correlation analysis was performed for LAI before and after correction for different methods. The corresponding figure plotting was completed in the software Sigmapolt v14.0 and Minitab v21.0.

3. Results

3.1. Effective LAI

The results of the effective LAI estimated by different methods were shown in Figure 3. The effective LAI estimated by all methods was larger than 2, and the maximum values estimated by LAI-2200, TRAC, and TLS multi-station were larger than 8. The data distributions of LAI-2200 and TLS multi-station were similar, with effective LAI mainly concentrated between 3 and 7. The data distributions of DHP and TLS single-station were similar, with effective LAI mainly concentrated between 3 and 5. The effective LAI estimated by TRAC was mainly concentrated between 5 and 7.
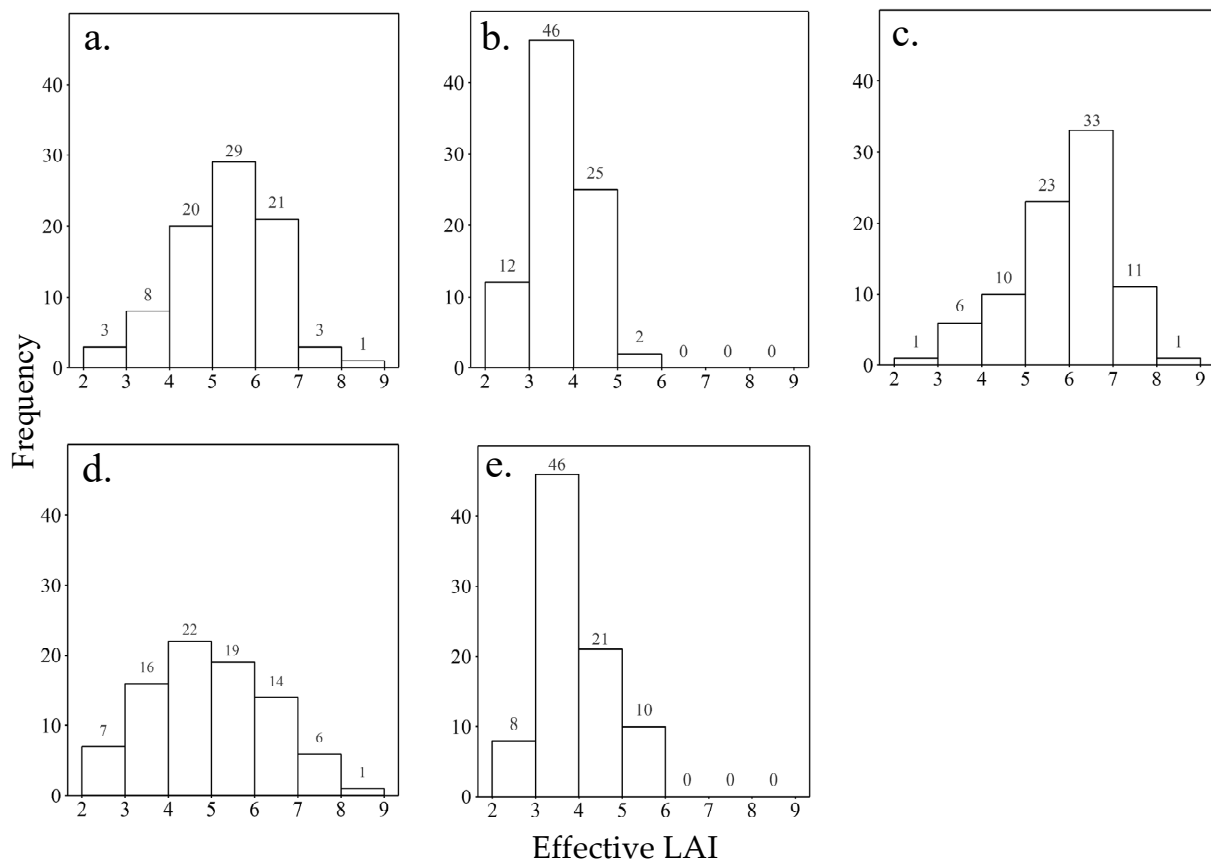
Figure 3. The distribution of effective LAI data estimated by different indirect methods. (**a**) LAI-2200; (**b**) DHP; (**c**) TRAC; (**d**) TLS1 (TLS multi-station); (**e**) TLS2 (TLS single-station).

A certain number of outliers existed in the effective LAI estimated by all methods (Figure 4a). The DHP and TLS single-station estimation results were significantly skewed from the mean (midway between the upper and lower box boundaries), showing a skew towards the lower boundary (25% quantile). It indicated that the observations of these two methods were generally concentrated in a low range. The observations of LAI-2200, TLS multi-station, and TRAC were in the high range and symmetrically distributed with the mean as the boundary. As shown in Figure 4b, the average effective LAI was 5.27 ± 1.16 (LAI-2200), 3.69 ± 0.74 (DHP), 5.86 ± 1.09 (TRAC), 4.93 ± 1.33 (TLS multi-station), and 3.87 ± 0.89 (TLS single-station). For the estimation of effective LAI, there was no significant difference between LAI-2200 and TLS multi-station, and no significant difference between DHP and TLS single-station. LAI-2200 was significantly different from DHP and TLS single station, respectively ($p < 0.05$), and TLS multi-station was significantly different from DHP and TLS single station, respectively ($p < 0.05$). There was a significant difference between TRAC and other methods ($p < 0.05$).

There was a significant correlation between the different methods (Table 2). LAI-2200 was significantly correlated with all other methods at the 0.01 level, with the strongest correlation with DHP ($r = 0.684$). DHP was significantly correlated with TRAC and TLS multi-station at the 0.05 level, respectively, and with TLS single-station at the 0.01 level ($r = 0.328$). TRAC was significantly correlated with TLS multi-station at the 0.05 level and with TLS single-station at the 0.01 level ($r = 0.283$). TLS multi-station was significantly correlated with TLS single-station at the 0.05 level ($r = 0.266$).
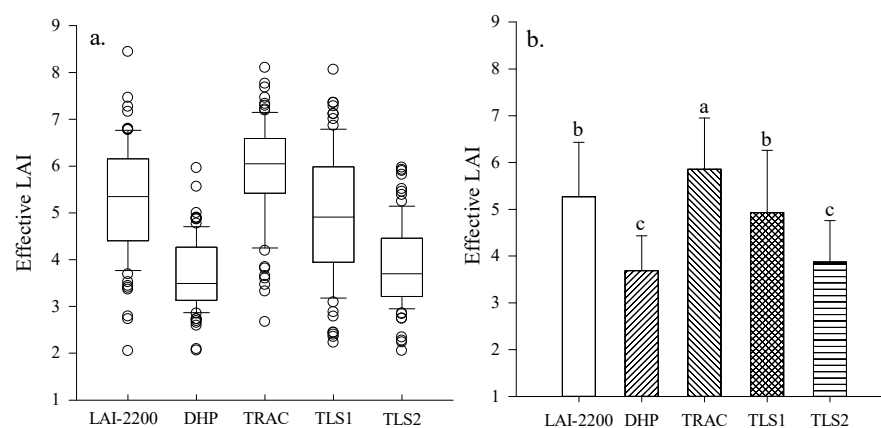
Figure 4. The difference of effective LAI estimated by different indirect methods. (**a**) Box plots, the central line in the box indicates the median, and the bottom and top edges indicate the 25th and 75th percentiles. Outliers are plotted using the "○" symbol; (**b**) Estimating performance (Mean ± SD). Different lowercase letters (a, b, or c) indicate significant differences between the effective LAI estimated by different methods ($p < 0.05$). TLS1 indicates TLS multi-station, and TLS2 indicates TLS single-station.

Table 2. Correlation coefficients of estimating the effective LAI by different indirect methods.

Method	LAI-2200	DHP	TRAC	TLS Multi-Station	TLS Single-Station
LAI-2200	1				
DHP	0.684 **	1			
TRAC	0.508 **	0.245 *	1		
TLS multi-station	0.599 **	0.254 *	0.249 *	1	
TLS single-station	0.493 **	0.328 **	0.283 **	0.266 *	1

*, $p < 0.05$; **, $p < 0.01$.

3.2. Correction Coefficient

The distribution of the correction coefficients for different sample plots was shown in Figure 5. The clumping index ranged from 0.73 to 1.00 with an average of 0.94 ± 0.05, and the data were relatively stable (the coefficient of variation was 5.32%). The woody-to-total area ratio ranged from 0.08% to 9.99%, with an average of 3.23 ± 2.22% and the data fluctuating (the coefficient of variation was 10.81%). The total correction coefficient ranged from 0.90 to 1.31, with an average of 1.03 ± 0.07. Therefore, if only the clumping effect and the wood component effect on the measurement were considered, the correct direction should be "upward". This indicated that "underestimation" occurred in the measurements of different methods. The degree of overestimation caused by the woody component was less than the degree of underestimation caused by the clumping effect. The clumping index was concentrated in the range of 0.92 to 1.00, accounting for 84.71% of the total number of samples. The woody-to-total area ratio was concentrated in the range of 0.08% to 5.00%, accounting for 82.35% of the total number of samples. The total correction coefficient was concentrated in the range of 0.90 to 1.10, accounting for 92.94% of the total number of samples. It was tested and found that there was no significant difference in the clumping index between the different sample plots (Figure 5a). Except for MZTX and MZTS, there was also no significant difference in woody proportions between the sample plots (Figure 5b). In general, it showed that the clumping intensity of leaves and canopy structure remained consistent between the different sample plots (Figure 5c).
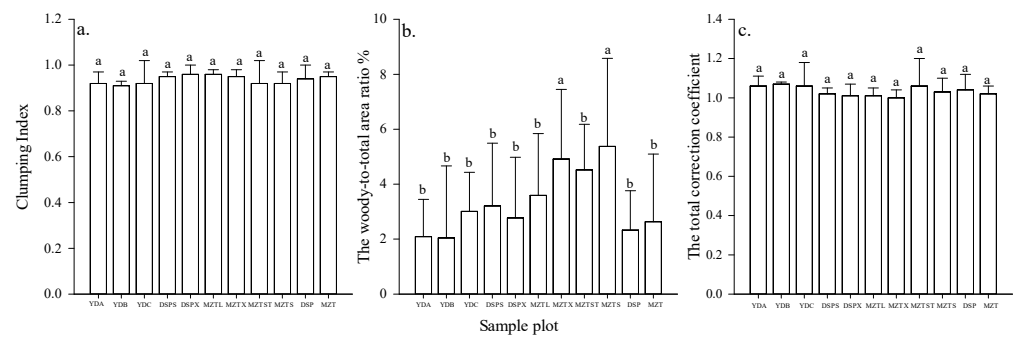
Figure 5. Correction coefficients for different sample plots. (**a**) Clumping Index; (**b**) The woody-to-total area ratio; (**c**) The total correction coefficient. Different lowercase letters (a, b) indicate significant differences between the correction coefficients of different sample plots ($p < 0.05$).

3.3. Corrected LAI

On the whole, the average of corrected LAI for LAI-2200, DHP, TRAC, TLS multi-station, and TLS single-station were 5.40 ± 1.19, 3.78 ± 0.75, 6.02 ± 1.14, 5.06 ± 1.39 and 3.97 ± 0.90, respectively. The data distributions for each method before and after correction were roughly the same. Although there was a corresponding increase in LAI after correction, there was no significant difference from that before correction (Figure 6). This was mainly because the clumping effect and the woody component had a similar degree of influence on the measurements.
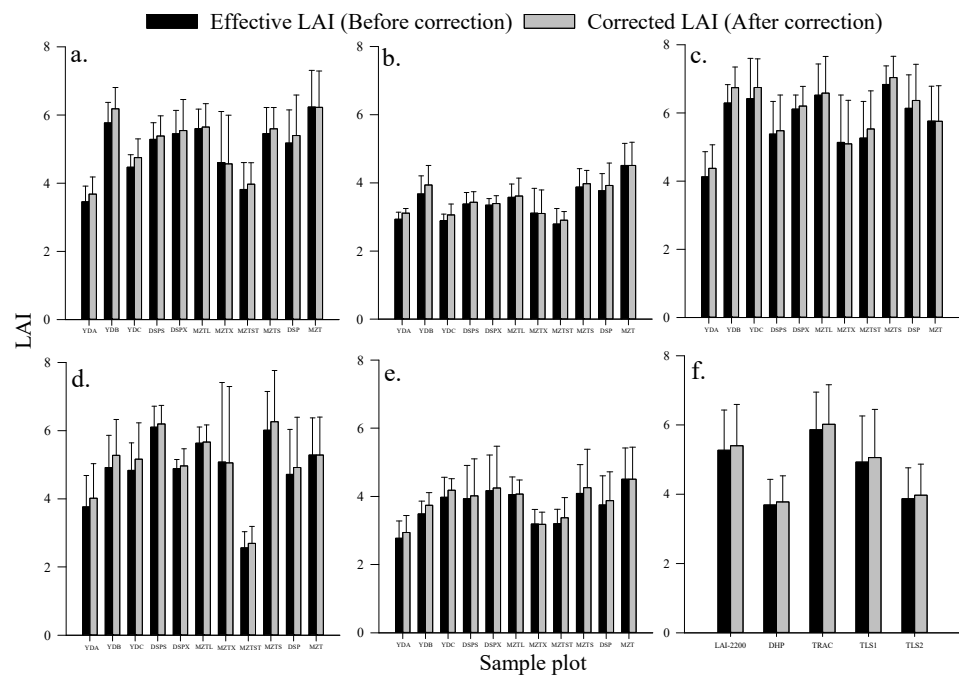

Figure 6. The estimated LAI before and after correction by different indirect methods (Mean $\pm$ SD). (**a**) LAI-2200; (**b**) DHP; (**c**) TRAC; (**d**) TLS1; (**e**) TLS2; (**f**) Total. TLS1 indicates TLS multi-station, and TLS2 indicates TLS single-station.

Compared to before correction, the correlations of the corrected LAI were enhanced for most methods (Table 3). For example, the correlation coefficients of LAI-2200 and TRAC, DHP and TLS multi-station, TRAC and TLS multi-station, and TLS multi-station and TLS single-station were improved. Especially, the significance level of TRAC and TLS multi-station was enhanced from 0.05 to 0.01 level. Therefore, the removal of clumping effects and woody components was still important to reduce measurement bias and uncertainty.

Table 3. Correlation coefficients of estimating the corrected LAI by different indirect methods.

Method	LAI-2200	DHP	TRAC	TLS Multi-Station	TLS Single-Station
LAI-2200	1				
DHP	0.682 **	1			
TRAC	0.511 **	0.249 *	1		
TLS multi-station	0.609 **	0.275 *	0.286 **	1	
TLS single-station	0.468 **	0.300 **	0.280 **	0.268 *	1

*, $p < 0.05$; **, $p < 0.01$.

4. Discussion

4.1. The LAI of the Tropical Forest

Although the true LAI was not obtained by the direct method for comparison in this study, and there were some differences in the effective LAI estimated by different methods, the results were in the range of 2 to 8, with the average value greater than 3.5. It confirmed that the tropical forest had a high LAI. Similarly, Behera et al. [9] reported a maximum LAI of 6.9 for tropical evergreen broad-leaved forests. Asner et al. [35] found that the LAI of tropical deciduous broad-leaved forests was 3.9 ± 2.5 on average and could reach a maximum LAI of 8.9. Wirth et al. [43] found that the LAI of tropical moist semideciduous forests ranged from 3 to 8, with an average LAI of 5.41 ± 0.82. Luo et al. [37] found that the LAI of Chinese forests was generally greater than 6 through modeling, especially in tropical rainforests and subtropical evergreen broad-leaved forests, with an average LAI of 6.29 in tropical evergreen broad-leaved forests. Clark et al. [44] and Qu et al. [45] concluded that the LAI of tropical forests had an average value of 6.0 at the regional scale and that the maximum LAI could reach 12.0. The results of this study were like the ones mentioned above, indicating that the LAI estimated by these methods was still effective. It was feasible to apply them to the northern tropical secondary monsoon rainforest.

4.2. Correction Effect

In this study, the woody component and clumping effect on the indirect method measurements were considered, and it was found that the corrected LAI was not significantly different from the effective LAI. Similarly, some studies also found that for broad-leaved forests, the effective PAI obtained by optical instruments was similar to the true LAI. On the one hand, correcting for woody components would remove the corresponding overestimation bias. On the other hand, correcting for clumping effects would also remove the corresponding underestimation bias, so these biases would compensate for each other in the correction process [46,47]. Many studies have shown that optical instruments that rely on gap fraction were prone to underestimate, especially in tropical dense forests where the optical band signal tended to saturate [8]. The overall direction of correction in this study was "upward", which justified the correction.

In addition, the accuracy of these correction coefficients needs to be ensured to obtain the desired correction results. On the one hand, there is still a large degree of uncertainty in determining the clumping index by using passive optical measurements [27,48]. The structure of leaf distribution in tropical forests is extremely complex, with multi-layered leaf alignment forms. Although the clumping index obtained by TRAC has been validated in many studies, most of them have been conducted in boreal forests and temperate forests [42,49], and measurements for tropical forests still need to be further tested. The average clumping index in this study was 0.94, slightly higher than the results measured in tropical forests by Padalia et al. [50] (0.82) and Tanaka et al. [51] (0.93), and future attempts could be made to select a more ideal condition for multiple replicate measurements.

On the other hand, the woody-to-total area ratio in humid tropical broadleaf forests was small, mainly because the leaf area was generally much larger than the branch area, most of the branches would be shaded by leaves, and the proportion of some stems and shoots was relatively small and negligible [52]. Olivas et al. [53] found that the woody-to-total area ratio in tropical rainforests was about 11%, while this study obtained an average

result of 3.23%, which was smaller overall. Besides the differences in forest structure, this was most likely related to the method of acquisition. In the evergreen forest, it was difficult to find a suitable season to apply the background method to directly obtain the wood area index [19]. In this study, woody components were manually removed from the images by the PS method, and the removal process was both tedious and somewhat subjective. The canopy leaves were dense and most of the trunk would also be shadowed by multiple layers of leaves (Figure 7); therefore, the use of a device that could quickly distinguish between green and non-green vegetation elements, such as a digital camera with several wavebands of imaging, would be a good direction for application. Such a device would further improve the applicability to various forest types.
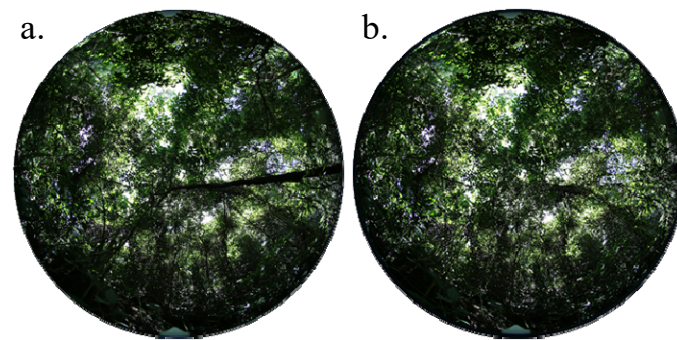

Figure 7. Treatment of woody components based on PS method. (**a**) original image; (**b**) processed image.

Meanwhile, we also found that the correlation of TLS single-station with LAI-2200, DHP, and TRAC was reduced after correction. The reason for this phenomenon may be related to the distribution from the original data of the different methods (Figure 4). On the one hand, the correction results of the different methods were obtained by multiplying the original data by the corresponding total correction coefficient (with an average of 1.03 ± 0.07). The original data of LAI-2200 and TRAC were much higher than the TLS single station, and the correction would expand their difference from the TLS single station. For example, the original data of one of the measurement points were 6.19 (LAI-2200), 5.82 (TRAC), and 3.10 (TLS single-station), with a total correction coefficient of 1.07, and the corrected results were 6.62 (LAI-2200), 6.23 (TRAC), and 3.32 (TLS single-station). On the other hand, the estimated value of the TLS single station was closer to the DHP, but the TLS single station had more outliers distributed in the range of 5–6, which also increased the difference between them after correction. The estimated results of the TLS multi-station were higher than the TLS single-station. Still, the TLS multi-station had more outliers distributed in the lower range (2–3), which greatly weakened the extreme bias of the correction. Therefore, the correlation between the corrected TLS multi-station and the TLS single-station was not reduced.

4.3. Measurement Comparisons and Problems

To make the obtained results more comparable, we let each method measure under a more ideal condition and kept almost the same position and measurement height. Although we took great care in the measurement scheme and operational steps and the different methods all rely on the gap fraction to achieve LAI inversion, there were still significant differences in the measurement results. It could be because the gap fraction was exponentially related to the LAI (Equation (1)), which could lead to large differences in LAI even if the deviations of the gap fraction obtained by different methods were small. In addition, this may also be related to differences in instrumental sensors and the sensitivity of the sensors to a complex canopy [13,26].

The sensors of the LAI-2200 and TRAC are linear (based on radiation). Because of the relatively small area measured, they were required to make multiple measurements at

different locations to adequately estimate canopy closure [54]. Even in a stable condition, the LAI-2200 is still susceptible to multiple reflections. When the LAI is greater than 2.5, specular reflection is more evident, resulting in the collected optical signal containing this "contribution" (overestimation of the gap fraction), which leads to an underestimation of the LAI (error of 20–25%) [24,55]. Nevertheless, compared to other traditional optical instruments, the LAI-2200 has shown that its estimated LAI is closest to the results obtained by the direct method [8,35]. It has 16-bit precision and keeps the sensitivity of light in a reasonable range by controlling the negative impact of direct light on the measurement. At the same time, the operator can also choose different view caps to adapt to the current measurement condition, making the operation more flexible. In contrast, TRAC is very dependent on direct sunlight when measuring LAI, but the direction of sunlight incidence is constantly changing at different times of the day. To obtain a relatively accurate LAI, it is necessary to ensure that a wide range of zenith angles is covered to receive the light signal [5,39]. In this study, the LAI estimated by TRAC was relatively high. This was most likely due to the large number of vines winding around the trees, which caused the direct light to be transformed into scattered light by different degrees of blockage during transmission and eventually underestimated the gap fraction.

The sensor of the DHP is an imaging sensor with a wide view angle (180°). Compared to the radiation sensor, it provides more detailed canopy information, but there are large deficiencies in measurement accuracy, which can lead to an underestimation of up to 50% in severe cases [19,23]. This was just as in this study, the LAI estimated by DHP was always in the low range. The overexposure problem and the classification threshold problem are the main sources of error in the DHP estimates of gap fraction and LAI [18,56]. On the one hand, overexposure increases the image brightness, which makes the canopy blurrier at the edges and reduces its optimal contrast with the sky. The bright canopy is easily mistaken for the sky and ignored in the calculation, and eventually, underestimation occurs. Therefore, it is necessary to properly consider the exposure settings of the camera and seek a balance between overexposure and underexposure. The automatic exposure mode was chosen for this study, which was likely to have some degree of overexposure problems, resulting in underestimation. On the other hand, accurate thresholds are the key to LAI calculation by DHP. The choice of manual threshold for the DHP by different operators resulted in up to a 17% range in gap fraction [57]. In this study, we obtained thresholds using Sidelook software, which eliminated subjective interpretation errors, but it was still necessary to compare their algorithms and recognition characteristics to reduce the influence of measurement results due to partial misclassification. In addition, the reason for the low measurement results of DHP may be related to the low pixel size of the camera used, and we could consider replacing the camera with a higher resolution for data acquisition in the future. Additionally, shaking might have occurred during the photo-taking process, which could have caused some of the photos to be not fully in focus, thus leading to the ignoring of more canopy details.

TLS is an active remote sensing technique that does not rely on visible light for its measurement. It does not need to consider the solar incidence direction, radiation type, and multiple reflections; therefore, it has great advantages in measuring different types of forest structure and secondary succession and can obtain more stable estimates, which should be theoretically superior to traditional optical methods [17,33]. When TLS is scanning, the trees behind in the same direction are easily shaded by the trees in front. The varying heights of the trees can make it easy for the lower canopy to shade out the higher canopy. At the same time, the number of acquired point clouds decreases as the scan radius increases, resulting in missing edges. In forests with higher LAI, such as LAI > 5, the shadowing effect becomes more significant [45]. In this study, the reason for the low results of TLS single-station estimation was still the shadowing effect, which made it difficult to obtain the complete canopy structure of trees. With multi-station measurements, TLS could obtain more "details" from multiple directions and compensate for the measurement bias caused by shadowing effects to the maximum extent, which was well reflected in the estimation

results of TLS multi-station (Figure 4). In addition, different algorithms and inversion models have important effects on the measurement results during the data processing of TLS. Some new methods, such as the voxel method [31], the path length distribution model [58], and the point space density (PSD) algorithm [25], were gradually used to improve their estimation of LAI in tropical forests. It is still an important research direction for TLS to choose a suitable algorithm to estimate LAI.

4.4. Other Uncertainties

Different ground-based indirect methods can generate methodological errors at any stage of model assumptions, sampling schemes, strategies, data collection, and analysis [59]. First, a key assumption is implicit in the use of gap fractions for LAI inversion: the projection functions (G, Equation (1)) are all considered to be essentially the same at the scene scale. Due to the difficulty of measuring the leaf angle distribution in practice, G is generally taken to be 0.5 to simplify the calculation [60]. However, it may also result in different degrees of error, which can be as high as 68% in severe cases [18,61]. Second, there is still no consistent agreement on the sampling strategy, scale, and frequency [26]. A reasonable sampling strategy can ensure the validity of the original data and maximize the performance of the instrument, but it also needs to take into account the height and vertical stratification of the canopy as well as spatial heterogeneity. Third, focus on the terrain effect. In mountainous areas with large surface relief (at slopes greater than 30°), topographic effects are likely to be an important error factor [62]. The gap fraction showed a significant asymmetric relationship at different slopes, which was mainly attributed to the difference in path length [58]. At the same time, a larger slope also increases the measurement difficulty and affects the stability of the instruments. Finally, forests are always in a constant state of development, with varying degrees of community succession, and it is still necessary to carry out long-term continuous location observations and verification work.

5. Conclusions

In this study, we attempted to compare the applicability of the LAI-2200, DHP, TRAC, and TLS methods for estimating the LAI of a typical northern tropical secondary monsoon rainforest. The TLS method was divided into single-station and multi-station measurements to analyze the effect of shadowing effects on its estimation of LAI. At the same time, the influence of the clumping effect and wood component on the measurements was quantified, and the effective LAI has been corrected accordingly. The main conclusions were as follows:

The measurement of LAI in dense evergreen tropical forests remained a considerable challenge. In this forest, the estimations of these ground-based methods did not show a high degree of agreement, although they were significantly correlated with each other. To meet the requirements for validating the satellite-derived products of LAI, there was still a need to further reduce the measurement differences between them.

Considering the stability and data collection efficiency, based on the results of this study, we advocated using the LAI-2200 method preferentially for LAI measurements in tropical forests to obtain more reliable estimates. The estimation of LAI using the DHP and TRAC methods was prone to underestimation and overestimation, respectively. Compared to the TLS single-station, the TLS multi-station could maximize the compensation for measurement bias due to shadowing effects. However, it was costly and cumbersome to process, which required a better solution to improve efficiency. Of course, the TLS single-station could also consider fusing airborne LiDAR data to reduce underestimation.

The existing correction methods seemed to be insufficient to fully correct the difference between these indirect methods. The clumping index and the woody-to-total area ratio were only able to compensate for the hypothetical deficiencies of the instrument. The measurement bias of these methods could be more due to the differences in sensor and instrument structures. In addition to obtaining these correction coefficients accurately, it was still necessary to get the true LAI as a correction reference using the direct methods.

Pay attention to the scaling effects. The results of this study were obtained using different ground-based methods for measurements at a plot scale of 10 m × 10 m. When they were used to validate remote sensing products, proper scaling conversion was required to match the pixel size.

References

1. Global Forest Resources Assessment 2020—Main Report. 2021. Available online: https://www.fao.org (accessed on 20 August 2022).
2. Olorunfemi, I.E.; Komolafe, A.A.; Fasinmirin, J.T.; Olufayo, A.A. Biomass carbon stocks of different land use management in the forest vegetative zone of Nigeria. *Acta Oecol.* **2019**, *95*, 45–56. [CrossRef]
3. Shennan-Farpón, Y.; Visconti, P.; Norris, K. Detecting ecological thresholds for biodiversity in tropical forests: Knowledge gaps and future directions. *Biotropica* **2021**, *53*, 1276–1289. [CrossRef]
4. Abbas, S.; Nichol, J.E.; Zhang, J.; Fischer, G.A.; Wong, M.S.; Irteza, S.M. Spatial and environmental constraints on natural forest regeneration in the degraded landscape of Hong Kong. *Sci. Total Environ.* **2021**, *752*, 141760. [CrossRef]
5. Yan, G.J.; Hu, R.H.; Luo, J.H.; Weiss, M.; Jiang, H.L.; Mu, X.H.; Xie, D.H.; Zhang, W.M. Review of indirect optical measurements of leaf area index: Recent advances, challenges, and perspectives. *Agric. For. Meteorol.* **2019**, *265*, 390–411. [CrossRef]
6. Parker, G.G. Tamm review: Leaf Area Index (LAI) is both a determinant and a consequence of important processes in vegetation canopies. *For. Ecol. Manag.* **2020**, *477*, 118496. [CrossRef]
7. Chen, J.M.; Black, T.A. Defining leaf area index for non-flat leaves. *Plant Cell Environ.* **1992**, *15*, 421–429. [CrossRef]
8. Fang, H.L.; Baret, F.; Plummer, S.; Schaepman-Strub, G. An overview of global leaf area index (LAI): Methods, products, validation, and applications. *Rev. Geophys.* **2019**, *57*, 739–799. [CrossRef]
9. Behera, S.K.; Behera, M.D.; Tuli, R. An indirect method of estimating leaf area index in a tropical deciduous forest of India. *Ecol. Indic.* **2015**, *58*, 356–364. [CrossRef]
10. Asaadi, A.; Arora, V.K.; Melton, J.R.; Bartlett, P. An improved parameterization of leaf area index (LAI) seasonality in the Canadian Land Surface Scheme (CLASS) and Canadian Terrestrial Ecosystem Model (CTEM) modelling framework. *Biogeosciences* **2018**, *15*, 6885–6907. [CrossRef]
11. Zeng, Y.; Hao, D.; Huete, A.; Dechant, B.; Berry, J.; Chen, J.M.; Joiner, J.; Frankenberg, C.; Bond-Lamberty, B.; Ryu, Y.; et al. Optical vegetation indices for monitoring terrestrial ecosystems globally. *Nat. Rev. Earth Environ.* **2022**, *3*, 477–493. [CrossRef]
12. Eriksson, H.; Eklundh, L.; Hall, K.; Lindroth, A. Estimating LAI in deciduous forest stands. *Agric. For. Meteorol.* **2005**, *129*, 27–37. [CrossRef]
13. Bréda, N.J. Ground-based measurements of leaf area index: A review of methods, instruments and current controversies. *J. Exp. Bot.* **2003**, *54*, 2403–2417. [CrossRef] [PubMed]
14. Srinet, R.; Nandy, S.; Patel, N.R. Estimating leaf area index and light extinction coefficient using Random Forest regression algorithm in a tropical moist deciduous forest, India. *Ecol. Inform.* **2019**, *52*, 94–102. [CrossRef]
15. Atkins, J.W.; Fahey, R.T.; Hardiman, B.S.; Gough, C.M. Forest canopy structural complexity and light absorption relationships at the subcontinental scale. *J. Geophys. Res. Biogeosci.* **2018**, *123*, 1387–1405. [CrossRef]
16. Schaefer, M.T.; Farmer, E.; Soto-Berelov, M.; Woodgate, W.; Jones, S. Overview of ground based techniques for estimating LAI. In *AusCover Good Practice Guidelines: A Technical Handbook Supporting Calibration and Validation Activities of Remotely Sensed Data Product*, 1st ed.; Held, A., Phinn, S., Soto-Berelov, M., Jones, S., Eds.; TERN AusCover: Brisbane, TAS, Australia, 2015; Volume 6, pp. 88–118.
17. Wang, Y.; Fang, H.L. Estimation of LAI with the LiDAR technology: A review. *Remote Sens.* **2020**, *12*, 3457. [CrossRef]

18. Woodgate, W.; Jones, S.D.; Suarez, L.; Hill, M.J.; Armston, J.D.; Wilkes, P.; Soto-Berelov, M.; Haywood, A.; Mellor, A. Understanding the variability in ground-based methods for retrieving canopy openness, gap fraction, and leaf area index in diverse forest systems. *Agric. For. Meteorol.* **2015**, *205*, 83–95. [CrossRef]

19. Liu, Z.L.; Chen, J.M.; Jin, G.Z.; Qi, Y.J. Estimating seasonal variations of leaf area index using litterfall collection and optical methods in four mixed evergreen–deciduous forests. *Agric. For. Meteorol.* **2015**, *209*, 36–48. [CrossRef]

20. Liu, Z.L.; Jin, G.Z.; Chen, J.M.; Qi, Y.J. Evaluating optical measurements of leaf area index against litter collection in a mixed broadleaved-Korean pine forest in China. *Trees* **2015**, *29*, 59–73. [CrossRef]

21. de Mattos, E.M.; Binkley, D.; Campoe, O.C.; Alvares, C.A.; Stape, J.L. Variation in canopy structure, leaf area, light interception and light use efficiency among Eucalyptus clones. *For. Ecol. Manag.* **2020**, *463*, 118038. [CrossRef]

22. Chen, J.M. Optically-based methods for measuring seasonal variation of leaf area index in boreal conifer stands. *Agric. For. Meteorol.* **1996**, *80*, 135–163. [CrossRef]

23. Zou, J.; Hou, W.; Chen, L.; Wang, Q.F.; Zhong, P.H.; Zuo, Y.; Luo, S.Z.; Leng, P. Evaluating the impact of sampling schemes on leaf area index measurements from digital hemispherical photography in *Larix principis-rupprechtii* forest plots. *For. Ecosyst.* **2020**, *7*, 52. [CrossRef]

24. Kuusk, A. Specular reflection in the signal of LAI-2000 plant canopy analyzer. *Agric. For. Meteorol.* **2016**, *221*, 242–247. [CrossRef]

25. Indirabai, I.; Nair, M.H.; Nair, J.R.; Nidamanuri, R.R. Direct estimation of leaf area index of tropical forests using LiDAR point cloud. *Remote Sens. Appl.* **2020**, *18*, 100295. [CrossRef]

26. Calders, K.; Origo, N.; Disney, M.; Nightingale, J.; Woodgate, W.; Armston, J.; Lewis, P. Variability and bias in active and passive ground-based measurements of effective plant, wood and leaf area index. *Agric. For. Meteorol.* **2018**, *252*, 231–240. [CrossRef]

27. Fang, H.L. Canopy clumping index (CI): A review of methods, characteristics, and applications. *Agric. For. Meteorol.* **2021**, *303*, 108374. [CrossRef]

28. Grotti, M.; Calders, K.; Origo, N.; Puletti, N.; Alivernini, A.; Ferrara, C.; Chianucci, F. An intensity, image-based method to estimate gap fraction, canopy openness and effective leaf area index from phase-shift terrestrial laser scanning. *Agric. For. Meteorol.* **2020**, *280*, 107766. [CrossRef]

29. Qi, Y.J.; Jin, G.Z.; Liu, Z.L. Optical and litter collection methods for measuring leaf area index in an old-growth temperate forest in northeastern China. *J. For. Res.* **2013**, *18*, 430–439. [CrossRef]

30. Liu, Z.L.; Jin, G.Z. Importance of woody materials for seasonal variation in leaf area index from optical methods in a deciduous needleleaf forest. *Scand. J. For. Res.* **2017**, *32*, 726–736. [CrossRef]

31. Vincent, G.; Antin, C.; Laurans, M.; Heurtebize, J.; Durrieu, S.; Lavalley, C.; Dauzat, J. Mapping plant area index of tropical evergreen forest by airborne laser scanning. A cross-validation study using LAI2200 optical sensor. *Remote Sens. Environ.* **2017**, *198*, 254–266. [CrossRef]

32. Wei, S.; Yin, T.; Dissegna, M.A.; Whittle, A.J.; Ow, G.L.F.; Yusof, M.L.M.; Lauret, N.; Gastellu-Etchegorry, J.P. An assessment study of three indirect methods for estimating leaf area density and leaf area index of individual trees. *Agric. For. Meteorol.* **2020**, *292*, 108101. [CrossRef]

33. Guo, X.X.; Wang, L.; Tian, J.Y.; Yin, D.M.; Shi, C.; Nie, S. Vegetation horizontal occlusion index (VHOI) from TLS and UAV image to better measure mangrove LAI. *Remote Sens.* **2018**, *10*, 1739. [CrossRef]

34. Pimmasarn, S.; Tripathi, N.K.; Ninsawat, S.; Sasaki, N. Applying lidar to quantify the plant area index along a successional gradient in a tropical forest of thailand. *Forests* **2020**, *11*, 520. [CrossRef]

35. Asner, G.P.; Scurlock, J.M.O.; Hicke, J.A. Global synthesis of leaf area index observations: Implications for ecological and remote sensing studies. *Glob. Ecol. Biogeogr.* **2003**, *12*, 191–205. [CrossRef]

36. Pfeifer, M.; Gonsamo, A.; Woodgate, W.; Cayuela, L.; Marshall, A.R.; Ledo, A.; Paine, T.C.E.; Marchant, R.; Burt, A.; Calders, K.; et al. Tropical forest canopies and their relationships with climate and disturbance: Results from a global dataset of consistent field-based measurements. *For. Ecosyst.* **2018**, *5*, 7. [CrossRef]

37. Luo, T.X.; Neilson, R.P.; Tian, H.Q.; Vörösmarty, C.J.; Zhu, H.Z.; Liu, S.R. A model for seasonality and distribution of leaf area index of forests and its application to China. *J. Veg. Sci.* **2002**, *13*, 817–830. [CrossRef]

38. Cao, M.; Zou, X.M.; Warren, M.; Zhu, H. Tropical forests of xishuangbanna, China. *Biotrop. J. Bio. Conserv.* **2006**, *38*, 306–309. [CrossRef]

39. Leblanc, S.G. Correction to the plant canopy gap-size analysis theory used by the Tracing Radiation and Architecture of Canopies instrument. *Appl. Opt.* **2002**, *41*, 7667–7670. [CrossRef]

40. Richardson, J.J.; Moskal, L.M.; Kim, S.H. Modeling approaches to estimate effective leaf area index from aerial discrete-return LIDAR. *Agric. For. Meteorol.* **2009**, *149*, 1152–1160. [CrossRef]

41. Fang, H.L.; Jiang, C.Y.; Li, W.J.; Wei, S.S.; Baret, F.; Chen, J.M.; Garcia-Haro, J.; Liang, S.L.; Liu, R.G.; Myneni, R.; et al. Characterization and intercomparison of global moderate resolution leaf area index (LAI) products: Analysis of climatologies and theoretical uncertainties. *J. Geophys. Res. Biogeosci.* **2013**, *118*, 529–548. [CrossRef]

42. Chen, J.M.; Rich, P.M.; Gower, S.T.; Norman, J.M.; Plummer, S. Leaf area index of boreal forests: Theory, techniques, and measurements. *J. Geophys. Res. Atmos.* **1997**, *102*, 29429–29443. [CrossRef]

43. Wirth, R.; Weber, B.; Ryel, R.J. Spatial and temporal variability of canopy structure in a tropical moist forest. *Acta Oecol.* **2001**, *22*, 235–244. [CrossRef]

44. Clark, D.B.; Olivas, P.C.; Oberbauer, S.F.; Clark, D.A.; Ryan, M.G. First direct landscape-scale measurement of tropical rain forest Leaf Area Index, a key driver of global primary productivity. *Ecol. Lett.* **2008**, *11*, 163–172. [CrossRef]

45. Qu, Y.H.; Shaker, A.; Silva, C.A.; Klauberg, C.; Pinagé, E.R. Remote sensing of leaf area index from LiDAR height percentile metrics and comparison with MODIS product in a selectively logged tropical forest area in Eastern Amazonia. *Remote Sens.* **2018**, *10*, 970. [CrossRef]

46. Schlerf, M.; Atzberger, C.; Hill, J. Remote sensing of forest biophysical variables using HyMap imaging spectrometer data. *Remote Sens. Environ.* **2005**, *95*, 177–194. [CrossRef]

47. Chen, J.M.; Mo, G.; Pisek, J.; Liu, J.; Deng, F.; Ishizawa, M.; Chan, D. Effects of foliage clumping on the estimation of global terrestrial gross primary productivity. *Glob. Biogeochem. Cycles* **2012**, *26*, GB1019. [CrossRef]

48. Gonsamo, A.; Pellikka, P. The computation of foliage clumping index using hemispherical photography. *Agric. For. Meteorol.* **2009**, *149*, 1781–1787. [CrossRef]

49. Ryu, Y.; Nilson, T.; Kobayashi, H.; Sonnentag, O.; Law, B.E.; Baldocchi, D.D. On the correct estimation of effective leaf area index: Does it reveal information on clumping effects? *Agric. For. Meteorol.* **2010**, *150*, 463–472. [CrossRef]

50. Padalia, H.; Sinha, S.K.; Bhave, V.; Trivedi, N.K.; Kumar, A.S. Estimating canopy LAI and chlorophyll of tropical forest plantation (North India) using Sentinel-2 data. *Adv. Space Res.* **2020**, *65*, 458–469. [CrossRef]

51. Tanaka, N.; Kume, T.; Yoshifuji, N.; Tanaka, K.; Takizawa, H.; Shiraki, K.; Tantasirin, C.; Tangtham, N.; Suzuki, M. A review of evapotranspiration estimates from tropical forests in Thailand and adjacent regions. *Agric. For. Meteorol.* **2008**, *148*, 807–819. [CrossRef]

52. Kucharik, C.J.; Norman, J.M.; Gower, S.T. Measurements of branch area and adjusting leaf area index indirect measurements. *Agric. For. Meteorol.* **1998**, *91*, 69–88. [CrossRef]

53. Olivas, P.C.; Oberbauer, S.F.; Clark, D.B.; Clark, D.A.; Ryan, M.G.; O'Brien, J.J.; Ordoñez, H. Comparison of direct and indirect methods for assessing leaf area index across a tropical rain forest landscape. *Agric. For. Meteorol.* **2013**, *177*, 110–116. [CrossRef]

54. Fassnacht, K.S.; Gower, S.T.; Norman, J.M.; McMurtric, R.E. A comparison of optical and direct methods for estimating foliage surface area index in forests. *Agric. For. Meteorol.* **1994**, *71*, 183–207. [CrossRef]

55. Ariza-Carricondo, C.; Di Mauro, F.; Roland, M.; Gielen, B.; Vitale, D.; Ceulemans, R.; Papele, D. A comparison of different methods for assessing leaf area index in four canopy types. *Cent. Eur. For. J.* **2019**, *65*, 67–80. [CrossRef]

56. Zhang, Y.; Chen, J.M.; Miller, J.R. Determining digital hemispherical photograph exposure for leaf area index estimation. *Agric. For. Meteorol.* **2005**, *133*, 166–181. [CrossRef]

57. Hancock, S.; Essery, R.; Reid, T.; Carle, J.; Baxter, R.; Rutter, N.; Huntley, B. Characterising forest gap fraction with terrestrial lidar and photography: An examination of relative limitations. *Agric. For. Meteorol.* **2014**, *189*, 105–114. [CrossRef]

58. Chen, Y.M.; Zhang, W.M.; Hu, R.H.; Qi, J.B.; Shao, J.; Li, D.; Wan, P.; Qiao, C.; Shen, A.J.; Yan, G.J. Estimation of forest leaf area index using terrestrial laser scanning data and path length distribution model in open-canopy forests. *Agric. For. Meteorol.* **2018**, *263*, 323–333. [CrossRef]

59. Jonckheere, I.; Fleck, S.; Nackaerts, K.; Muys, B.; Coppin, P.; Weiss, M.; Baret, F. Review of methods for in situ leaf area index determination: Part I. Theories, sensors and hemispherical photography. *Agric. For. Meteorol.* **2004**, *121*, 19–35. [CrossRef]

60. Leblanc, S.G.; Fournier, R.A. Hemispherical photography simulations with an architectural model to assess retrieval of leaf area index. *Agric. For. Meteorol.* **2014**, *194*, 64–76. [CrossRef]

61. Hu, R.H.; Yan, G.J.; Nerry, F.; Liu, Y.S.; Jiang, Y.M.; Wang, S.R.; Chen, Y.M.; Mu, X.H.; Zhang, W.M.; Xie, D.H. Using airborne laser scanner and path length distribution model to quantify clumping effect and estimate leaf area index. *IEEE Trans. Geosci. Remote Sens.* **2018**, *56*, 3196–3209. [CrossRef]

62. Gonsamo, A.; Pellikka, P. Methodology comparison for slope correction in canopy leaf area index estimation using hemispherical photography. *For. Ecol. Manag.* **2008**, *256*, 749–759. [CrossRef]